Communications to the Editor

Morphology and Miscibility of Blends of Ethylene−Tetrafluoroethylene Copolymer/ Poly(methyl methacrylate) Studied by ToF SIMS Imaging

Lu-Tao Weng,† Terry L. Smith,† Jiyun Feng,‡ and Chi-Ming Chan*,‡

Materials Characterization and Preparation Center, Department of Chemical Engineering and Advanced Engineering Materials Facility, Hong Kong University of Science & Technology, Clear Water Bay, Kowloon, Hong Kong

Received December 27, 1996
Revised Manuscript Received September 29, 1997

Introduction. One of the most important issues in the study of polymer blends is miscibility.[1−3] Up to now, information about polymer miscibility has typically been obtained from the glass transition temperature measurements. A single T_g is observed when two polymers are miscible (domain size < 15 nm),[3] whereas when two polymers are completely immiscible, their T_gs remain unchanged. In a study of the ethylene−tetrafluoroethylene copolymer (ETFE)/poly(methyl methacrylate) (PMMA) blends, three glass transition temperatures were observed.[4] The low (∼46 °C) and high (∼105 °C) T_gs correspond to the semicrystalline ETFE phase (with a very small amount of PMMA) and the PMMA amorphous phase (with a small amount of ETFE), respectively. The intermediate T_g (∼65 °C) is associated with an amorphous phase containing significant levels both of ETFE and PMMA (ETFE/PMMA phase). Using the Fox equation, the weight fraction of ETFE in this phase was estimated to be approximately 0.55. The detection of the low and high T_gs is relatively straightforward from the use of techniques such as differential scanning calorimetry (DSC) and dynamical mechanical analysis (DMA). However, the intermediate T_g appears as a very weak transition in the DSC scans, and its presence is overshadowed by a very broad β transition of PMMA in the DMA curves. It is important to point out that the presence of this intermediate T_g is barely detectable by DSC for the blends obtained by slowly cooling the samples from the melts and that its detectability is enhanced if the blends are quenched from their melts.

The physical and chemical properties of polymer blends and copolymers have been studied by surface analysis techniques such as X-ray photoelectron spectroscopy (XPS) and static secondary ion mass spectrometry (SSIMS).[5−22] Recently, time-of-flight secondary ion mass spectrometry (ToF SIMS) has been used to study the morphology of polymer blends.[19] When this is coupled with a liquid metal ion gun, surface chemical imaging with submicron lateral resolution is possible for polymeric materials. In the present work, this imaging capability is used to study the surface morphology of the partially miscible blends of ETFE/PMMA. For the ETFE/PMMA system, we should be able to locate three regions—a semicrystalline region containing mostly ETFE with a T_g close to that of pure ETFE, an amorphous region containing mostly PMMA with a T_g close to that of pure PMMA, and an amorphous region containing significant levels of ETFE and PMMA.

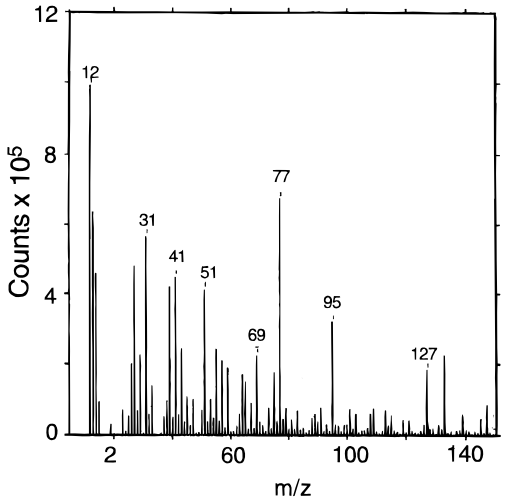

Figure 1. Positive ToF SIMS spectrum of pure ETFE.

Experimental Section. The ETFE used in this study is an alternating ethylene−tetrafluoroethylene copolymer supplied by Du Pont. The PMMA was purchased from Scientific Polymer Products Inc. The inherent viscosity of the PMMA is 0.45. ETFE/PMMA blends were prepared by a Haake Rheocord mixer 9000 at 280 °C for 10 min. Two blend compositions, ETFE/PMMA = 20/80 and 40/60 (in weight percentages), were studied. Sheets of thickness of about 1.5 mm were prepared using a hot press at 250 °C. Then the sample was slowly cooled in the press under pressure by compressed air after the power had been turned off. Another set of samples was prepared by quenching the polymer melt into ice water. To obtain a flat surface for ToF SIMS analysis, the samples were prepared by a cryomicrotome at −100 °C. The morphology of the surface of the samples is expected to be identical to that of the bulk because the T_gs of ETFE and PMMA are higher than ambient temperature.

ToF SIMS measurements were performed on a Physical Electronics PHI 7200 ToF SIMS spectrometer equipped with two ion guns (Cs^+ for high mass resolution spectroscopy and $^{69}Ga^+$ for spatially resolved imaging) and a reflectron ToF analyzer. The detailed descriptions and performances of this instrument have been reported previously.[23,24] In this work, the images were acquired in both positive and negative modes using

* To whom correspondence should be addressed.
† Materials Characterization and Preparation Center.
‡ Department of Chemical Engineering and Advanced Engineering Materials Facility.

S0024-9297(96)01916-X CCC: $15.00
Published on Web 01/24/1998

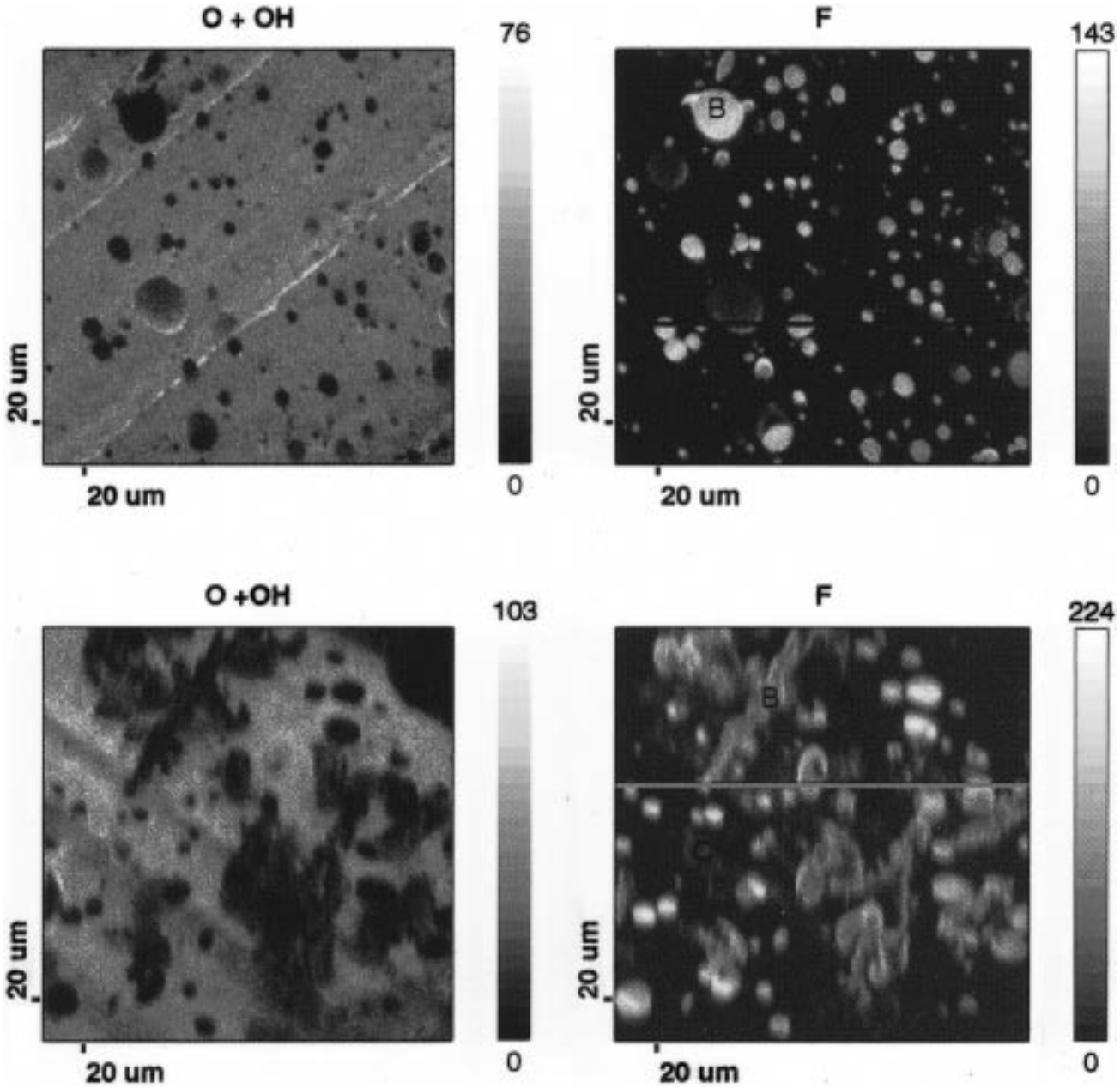

Figure 2. Negative ToF SIMS images obtained for two samples with a blend composition of ETFE/PMMA = 20/80. The upper and lower images are for the slowly cooled and quenched samples, respectively. Imaged area is 200 μm × 200 μm.

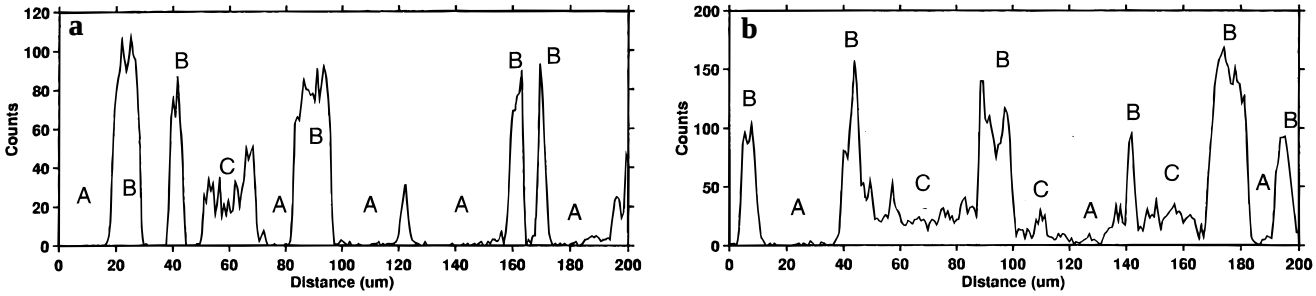

Figure 3. Line scans for F^- (represented by the blue lines in the F^- images, as shown in Figure 2) for the slowly cooled (a) and quenched samples (b).

a $^{69}Ga^+$ beam operating at 25 keV. To obtain high spatial resolution images and easy control of surface charge stabilization, an ion pulse length of about 20 ns was used. In this case, each pulse delivered about 125 ions and the measured beam size was ~0.5 μm. The time to digital converter was 10 ns. The imaged area was 200 × 200 μm (256 × 256 pixels). The complete image was acquired from up to a maximum of 200 frame scans using one primary ion pulse per pixel, corresponding to the total ion dose of lower than 4×10^{12} ions/cm^2. Charge compensation was achieved with a pulsed low-energy (0−70 eV) flooding electron gun (the pulses

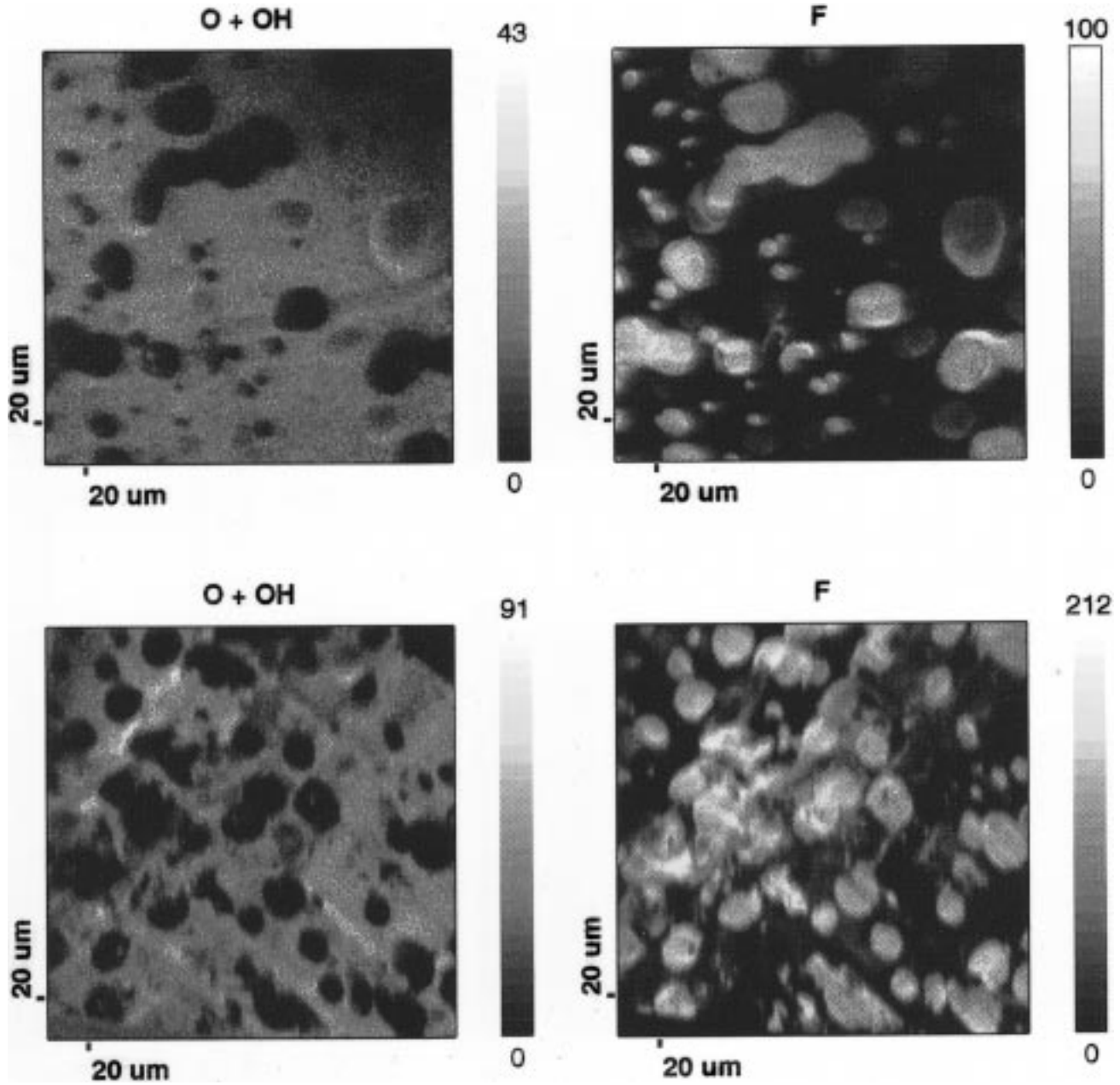

Figure 4. Negative ToF SIMS images obtained for the sample with a blend composition of ETFE/PMMA = 40/60. Upper and lower images are the slowly cooled and quenched samples, respectively. Imaged area is 200 μm × 200 μm.

are out of phase from those of the primary ion beam). The data in this work were acquired in the so-called "raw data stream" mode.[24] In this mode, the full spectral information at every pixel was stored to create a complete raw data stream for each image. An image from a selected peak (or a group of peaks) and the spectra from a selected image area can be created.

Results and Discussion. Before ToF SIMS imaging, the fingerprint spectra of both ETFE and PMMA were obtained by using an 8 keV Cs^+ ion gun (mass resolution about 7000). The SIMS spectra of PMMA are similar to those published previously with the most characteristic fragments at m/z = 15 (CH_3^+), 59 ($C_2H_3O_2^+$), 69 ($C_4H_5O^+$), etc. in positive polarity and m/z = 16/17 (O^-/OH^-), 31 (CH_3O^-), 55 ($C_3H_3O^-$), 85 ($C_4H_5O_2^-$), etc. in negative polarity.[25] Figure 1 shows a positive spectrum of ETFE. The most characteristic fragments are at m/z = 12 (C^+), 31 (CF^+), 51 (CHF_2^+), 59 ($C_2H_4F^+$), 69 (CF_3^+), 77 ($C_3H_3F^+$), 95 ($C_3H_2F_3^+$), and 127 ($C_4H_4H_3^+$, deprotonated monomer). The negative spectrum of ETFE is totally dominated by the peak at m/z = 19 (F^-), with some other small characteristic fragments at m/z = 31 (CF^-), 38/39 (F_2^-/F_2H^-), and 43 (C_2F^-). In principle, the above fragments can be used to monitor the distribution of PMMA and ETFE. However, as the mass resolution was only moderate in the imaging mode, certain fragments of PMMA cannot be used because they overlap the fragments of ETFE (e.g. at m/z = 59, $C_2H_3O_2^+$ of PMMA overlaps with $C_2H_4F^+$ of ETFE). Some other fragments cannot be used due to their low intensities in the blends. In the following, only the O^-/OH^- images representing PMMA and F^- images representing ETFE are presented in the negative mode. In the positive mode, the ETFE is represented by $C_3H_3F_2^+$ and $C_3H_2F_3^+$, and PMMA is represented by CH_3^+.

Figure 2 displays the O^- + OH^- and F^- images for the blend (ETFE/PMMA = 20/80). The upper and lower

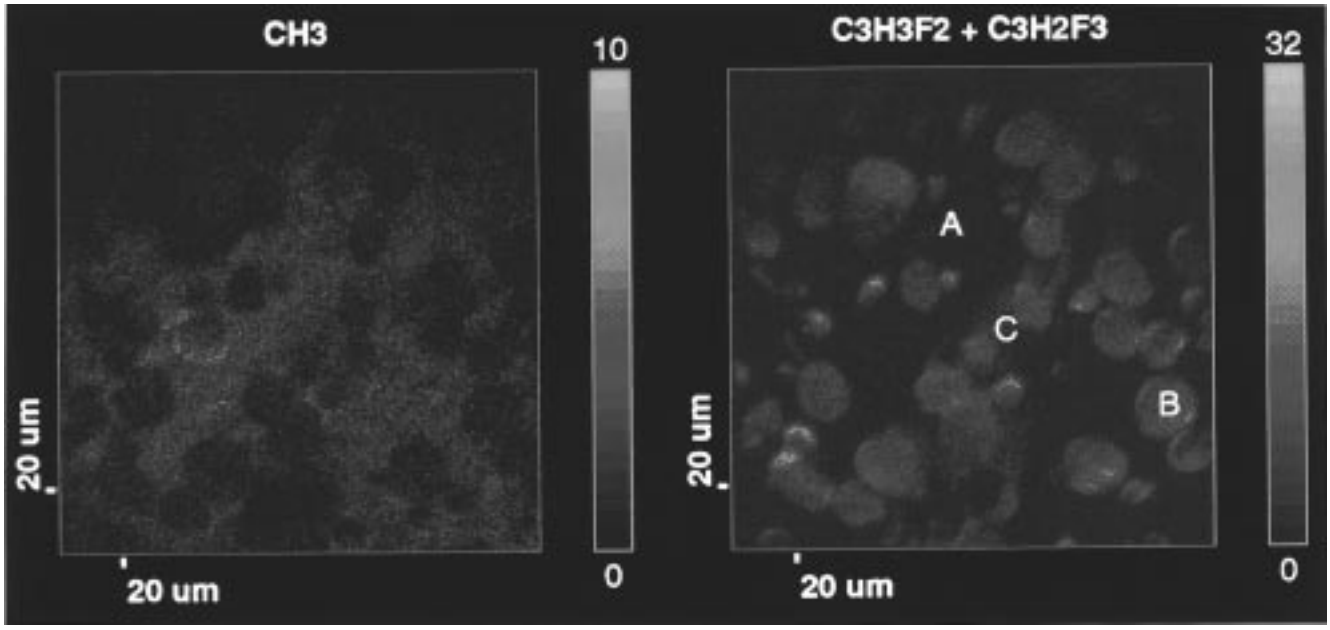

Figure 5. Positive ToF SIMS images obtained with molecular fragments (a) CH_3^+ and (b) $C_3H_3F_2^+ + C_3H_2F_3^+$, for a quenched sample (ETFE/PMMA = 40/60).

images are for the sample prepared by slow cooling and quenching, respectively. The $O^- + OH^-$ and F^- images are complementary. For the slowly cooled sample, the ETFE particles (phase B) are dispersed in the PMMA matrix (phase A). In most cases, the particles are well defined with the size ranging from about 1 μm to 20 μm. Spectra are reconstructed using data obtained from phases A and B. The fragments from phases A and B are close to those for PMMA and ETFE, respectively. However, the intensities of the $O^- + OH^-$ peaks are not zero in phase B and the intensity of the F^- peak is not zero in phase A. These results show that there is a small amount of PMMA and ETFE in phases B and A, respectively. In addition, a small amount of a phase (phase C) that contains high levels of ETFE and PMMA can also be detected. Both PMMA and ETFE fragments are present in the spectrum reconstructed from phase C. These results are in agreement with the DSC measurements.[4] For the quenched sample, the surface morphology is quite different, as shown in Figure 2 (lower images). Although the dispersion of the ETFE particles in the PMMA matrix is still observed, a much large amount of phase C is detected.

The line scans, the locations of which are marked by blue lines in the F^- images (as shown in Figure 2), are displayed in Figure 3a. It can be observed that for the slowly cooled sample, two phases are present—the F^- signal is either almost zero in phase B or very high in phase A. A small amount of phase C is also detected. For the quenched sample, however, a large amount of phase C is observed in the regions between the ETFE particles, as shown in Figure 3b. Very similar situations can be observed from the images presented in Figure 4 for the blend (ETFE/PMMA = 40/60). Again, the upper and lower images are obtained with the slowly cooled and quenched samples, respectively. In this blend (ETFE/PMMA = 40/60), one can observe that the ETFE particles are larger. In comparing the slowly cooled with the quenched samples, the C phase, which does not have a well-defined shape, is again observed easily in the quenched sample. The above results obtained in the negative polarity are confirmed with those obtained in the positive polarity. Figure 5 displays the images obtained with the molecular fragments at $m/z = 15$ (CH_3^+) (representing PMMA phase) and 77 ($C_3H_3F_2^+$) + 95 ($C_3H_2F_3^+$) (representing the ETFE phase) for the blend (ETFE/PMMA = 40/60) quenched from the melt. It can be observed that both images shown in Figure 5 are complementary. Most importantly, similar to the negative images, three phases (as indicated in the Figure 5) are present in this sample.

Conclusions. ToF SIMS imaging capability has been successfully used to study the morphology and miscibility of the ETFE/PMMA blends. A semicrystalline region containing mostly ETFE, an amorphous region containing mostly PMMA and an amorphous region containing significant levels of ETFE and PMMA were detected. These results are in total agreement with the DSC measurements. In this study, ToF SIMS imaging technique has been shown to be a powerful tool to study the polymer morphology and miscibility of polymer blends provided that the polymers have distinct characteristic fragments.

Acknowledgment. This work was supported by the Hong Kong Government Research Grant Council under Grant No. HKUST 6123/97P.

References and Notes

(1) Paul, D. R.; Newman, S. *Polymer Blends*; Academic Press: New York, 1978; Vols. 1 and 2.
(2) Olabish, O.; Robson, M.; Shaw, M. T. *Polymer-Polymer miscibility*; Academic Press: New York, 1979.
(3) Utracki, L. A. *Polymer Alloys and Blends*; Hanser Publishers, Munich, Germany, 1989.
(4) Feng, J.; Chan, C.-M. *Polymer* **1997**, *38*, 6371.
(5) Chan, C.-M. *Polymer Surface Modification and Characterization;* Hanser: New York, 1994.
(6) Chen, X.; Gardella, J. A., Jr.; Ho, T.; Wynne, K. J. *Macromolecules* **1995**, *28*, 1635.
(7) Schmidt, J. J.; Gardella, J. A., Jr.; Salvati, L., Jr. *Macromolecules* **1989,** *22*, 4489.
(8) Zhuang, H.; Gardella, J. A., Jr. *Macromolecules* **1997**, *30*, 3632.
(9) Kumler, P. L.; Matteson, H. L.; Gardella, J. A., Jr. *Langmuir* **1991**, *7*, 2479.

(10) Gardella, J. A., Jr. *Appl Surf. Sci.* **1998**, *31*, 72.
(11) Boyd, R. D.; Badyal, J. P. S. *Macormolecules* **1997**, *30*, 3658.
(12) Lhoest, J. B.; Bertrand, P.; Weng, L. T.; Dewez, J. L. *Macromolecules* **1995**, *28*, 4631.
(13) Affrossman, S.; Bertrand, P.; Hartshorne, M; Kiff, T.; Leonard, D.; Pethrick, R. A.; Richards, R. W. *Macromolcules* **1996**, *29*, 5432.
(14) Patel, N. W.; Dwight, D. W.; Hedrick, J. L.; Webster, D. C.; McGrath, J. E. *Macromolecules* **1988**, *21*, 2698.
(15) Inoue, H.; Matsumoto, A.; Matsukawa, K.; Ueda, A.; Nagai, S. *J. Appl. Polym. Sci.* **1990**, *40*, 1917.
(16) Inoue, H.; Matsumoto, A.; Matsukawa, K.; Ueda A.; Nagai, S. *J. Appl. Polym. Sci.* **1990**, *41*, 1815.
(17) McMaster, L. P. *Macromolecules* **1978**, *11*, 1973.
(18) Qamardeep, S. B.; Pan, D. H.; Koberstein, J. T. *Macromolecules* **1988**, *21*, 2166.
(19) Briggs, D.; Fletcher, I. W.; Reichlmaier, S.; Agulo-Sanchez, J. L.; Short, R. D. *Surf. Interface Anal.* **1996**, *24*, 419.
(20) Li, L.; Chan, C.-M.; Weng, L. T. *Macromolecules* **1997**, *30*, 3698.
(21) Briggs, D. In *Practical Surface Analysis, Vol 2, Ion and Neutral Spectroscopy*; Briggs, D., Seah, M. P., Eds.; Wiley: Chichester, England, 1990; p 307.
(22) Benninghoven, A. *Angew. Chem. Int. Ed. Engl.* **1994**, *33*, 1023.
(23) Reichlmaier, S.; Hammond, J. S.; Hearn, M. J.; Briggs, D. *Surf. Interface Anal.* **1994**, *21*, 739.
(24) Reichlmaier, S.; Bryan, S. R.; Briggs, D. *J. Vac. Sci. Technol. A* **1995**, *13*, 1217.
(25) Hearn, M. J.; Briggs, D., *Surf. Interface Anal.* **1988**, *11*, 198.

MA961916M